Novel observables for exploring QCD collective evolution and quantum entanglement within individual jets

Austin Baty,[*] Parker Gardner,[†] and Wei Li[‡]
Department of Physics and Astronomy, Rice University, 6100 Main St., Houston, Texas 77005, USA

(Received 24 May 2022; revised 15 May 2023; accepted 30 May 2023; published 23 June 2023)

We postulate that nonperturbative quantum chromodynamics (QCD) effects occurring during parton fragmentation can result in collective effects of a multiparton system, reminiscent of those observed in high-energy hadronic or nuclear interactions with large final-state particle multiplicity. Proton-proton collisions at the CERN Large Hadron Collider showed surprising signatures of a strongly interacting, thermalized quark-gluon plasma, which was thought only to form in collisions of large nuclear systems. Another puzzle observed earlier in e^+e^- collisions is that production yields of various hadron species appear to follow a thermal-like distribution with a common temperature. We propose searches for thermal and collective properties resulting from parton fragmentation processes using high multiplicity jets in high-energy elementary collisions. Several novel observables are studied using the PYTHIA 8 Monte Carlo event generator. Experimental observation of such collectivity will offer a new view of nonperturbative QCD dynamics of multiparton systems at the smallest scales. Absence of any collective effects may offer new insights into the role of quantum entanglement in the observed thermal behavior of particle production in high energy collisions.

DOI: 10.1103/PhysRevC.107.064908

I. INTRODUCTION

Quantum chromodynamics (QCD) is the fundamental theory that describes properties of quarks and gluons (known as partons) and the interactions among them. Being an $SU(3)$ non-Abelian gauge theory, QCD has the peculiar feature that partons interact strongly at long distances, but become almost free when close to each other ("asymptotic freedom") [1–3]. As a consequence, no free partons are ever found in the vacuum. Instead, partons are always confined inside hadrons. Attempts to knock a parton out of a hadron and into the vacuum (e.g., via a hard scattering in high-energy proton collisions) lead to the emission of collimated sprays of hadrons (or "jets") that result from fragmentation and hadronization of the scattered parton. Detailed dynamics of the parton fragmentation and hadronization process are not yet fully understood and cannot be evaluated from first-principles because of QCD's nonperturbative nature. Phenomenological models such as the Lund string [4] and cluster models [5] have been implemented to facilitate the interpretation of experimental data. In recent years, there has been tremendous interest and progress in the study of jet substructures [6]. In these studies, perturbative QCD (pQCD) approaches have been successfully applied by largely avoiding or trimming away nonperturbative components (i.e., soft particles) of the jet [6]. Fundamental understandings of *color confinement* and the *dynamics of hadronization* are two key outstanding issues in QCD and strong interactions.

Experiments studying high-energy heavy nucleus collisions have been carried out to overcome the QCD confinement and create (possibly thermalized) matter with quark-gluon degrees of freedom over an extended space-time dimension. Lattice QCD theory predicts that a crossover transition to a new phase of partonic matter, known as the *quark-gluon plasma* (QGP), occurs at a temperature of about 157 MeV near zero baryon chemical potential [7–9]. In a high-energy nucleus-nucleus (AA) collision (e.g., Au or Pb ion), the large volume and density of initial partons can lead to many rescatterings, which may rapidly drive the system toward a thermalized QGP state. Over the past decades, experiments at the CERN Super Proton Synchrotron (SPS) [10], BNL Relativistic Heavy Ion Collider (RHIC) [11–14], and CERN Large Hadron Collider (LHC) [15] have provided compelling evidence for the formation of hot and dense QGP matter. Striking long-range collective phenomena have been observed and extensively studied using the azimuthal correlations of particles emitted over a wide pseudorapidity range (also known as the "Ridge") at RHIC [16–19] and the LHC [20–24]. These observations indicate that QGP matter is strongly coupled and exhibits the hydrodynamic behavior of a nearly perfect liquid [25–29].

It was thought that elementary collision systems such as e^+e^-, proton-proton, etc., were too small and dilute for any

[*]abaty@rice.edu
[†]ptg2@rice.edu
[‡]wl33@rice.edu

secondary partonic rescattering to occur and drive the system toward equilibrium. For this reason, collective flow behavior from a QGP medium was not expected in these systems. Surprisingly, since the start of the LHC, similar long-range collective azimuthal correlations have been discovered in proton-proton (pp) collisions with large final-state particle multiplicity [30–34], which raised the question of whether a tiny QGP droplet with a significantly smaller size is created [35]. Subsequently, such collective phenomena have been observed in additional small systems, such as proton-nucleus (pA) [36–45] and lighter nucleus-nucleus systems [45–48] at RHIC and the LHC. While it is widely accepted that strong final-state partonic rescatterings do play a prominent role in the observed collectivity of small, high-multiplicity systems, questions remain whether the rescatterings are strong enough to drive the system close to equilibrium or a domain where hydrodynamics is applicable. Meanwhile, alternative scenarios based on gluon saturation in the initial state may also contribute, especially at lower particle multiplicities (see reviews and latest developments in Refs. [49–51]).

It is evident that collective effects of strongly correlated partonic systems are not only limited to those created in large AA collisions. Therefore, a series of compelling questions arise: *From how small of a system can partonic collectivity emerge and under what conditions? Is partonic collectivity at such small scales unexpected or a natural consequence of QCD in its nonperturbative regime? Can hydrodynamics be an effective tool in describing nonperturbative QCD dynamics of many-body partonic systems (e.g., fragmentation in the vacuum)?*

In fact, it has been pointed out long ago that total production yields of various hadron species in elementary e^+e^- collisions can be well described by a thermal statistical model [52–54], similar to that in large AA collisions from a nearly thermalized QGP medium [55]. The origin of this thermal-like phenomenon in e^+e^- has not been understood, as it was inconceivable that strong final-state partonic rescatterings occur there. There are conjectures that thermal-like hadron production is the QCD counterpart of Hawking-Unruh radiation [54,56,57]. In recent years, quantum entanglement effects were also proposed to give an intriguing alternative perspective of multiparticle production in high-energy collisions [58–62]. The apparent thermalization of final-state hadrons in e^+e^- may be related to dynamics of an expanding quantum string stretched between the quark-antiquark pair and its subsequent quenching [59]. No secondary partonic scatterings are involved in this explanation. In these models entanglement entropy is calculated with an effective thermal temperature and can be related to the temperature extracted by fitting identified hadron multiplicities to thermal statistical models.

Recent experimental searches for long-range ridge correlations in e^+e^- [63] or e^-p collisions [64] have yielded null results so far, seeming to support the absence of strong final-state rescatterings. However, in these studies the event multiplicity reach is rather limited (up to $\approx$30 tracks in each event), so the presence of rescatterings in small systems achieving higher final-state particle densities can not be ruled out by these data. As will be discussed further, a single high-multiplicity jet is an example of a small system which may be able to extend the search for final-state rescattering effects to much higher values of local particle density.

Motivated by earlier experimental and theoretical work, our purpose in this paper is to discuss the possibility of understanding the fundamental questions and puzzles outlined above from a different view. In particular, we postulate that a strongly interacting, QGP-like state[1] can indeed originate from a fragmenting quark or gluon as it propagates through the QCD vacuum. As a natural consequence of the intrinsic strong QCD coupling strength, the strong color fields of the primordial parton in the vacuum can give rise to a large number of secondary partons. These partons subsequently interact and develop collective expansion which is transverse to the original parton's direction of motion and extends over a finite space-time volume. We lay out a proposal to examine a series of key signatures (e.g., long-range azimuthal correlations) of such potential QGP-like states using energetic jets copiously produced in pp collisions at the present CERN LHC, and also at potential future pp, e^-p, and e^+e^- colliders. Similar studies are also applicable in nuclear collisions to explore the "expansion" of a parton in a colored medium, instead of the vacuum. Observation of QGP-like signatures for a fragmenting parton will provide new insights to the "thermal" behavior seen from e^+e^- to AA collisions, and potentially allow a unified view of non-perturbative many-body QCD processes (e.g., hydrodynamics models). Conversely, the absence of those collective signatures may highlight the role of quantum entanglement effects in parton fragmentation and hadronization. The direction of research explored by this study shares strong synergy with both the jet substructure and relativistic heavy ion communities.

The paper is organized in the following way. Section II outlines the underlying idea of the possible formation of "QGP" from a parton propagating in the vacuum. Section III discusses specific key signatures and how to search for them experimentally using Monte Carlo (MC) generators for demonstration. Section IV is devoted to more physics discussions and extension of proposed studies to other future directions. The paper ends with a summary in Sec. V.

II. SINGLE-PARTON "QGP" IN THE VACUUM

In the QCD vacuum state, the chiral symmetry is spontaneously broken because of the strong coupling nature at low energies. The QCD vacuum is not empty but filled with nonvanishing condensates of quark-antiquark pairs ($\langle\bar{q}_L q_R\rangle + \langle\bar{q}_R q_L\rangle$) and gluons ($\langle G_{\mu\nu}G^{\mu\nu}\rangle$), or chiral condensates. As a thought experiment, consider an extreme (although unrealistic) situation, where a single parton is placed at rest in the vacuum, as illustrated in Fig. 1 (top). The potential energy of associated color fields is infinite. Consequently, more quark-antiquark pairs and gluons will be immediately excited out of the surrounding condensate sea. Thus, in the vicinity of the

[1]"QGP-like" refers to the state where qualitative signatures of partonic collectivity are present but the system does not necessarily reach the hydrodynamic limit.

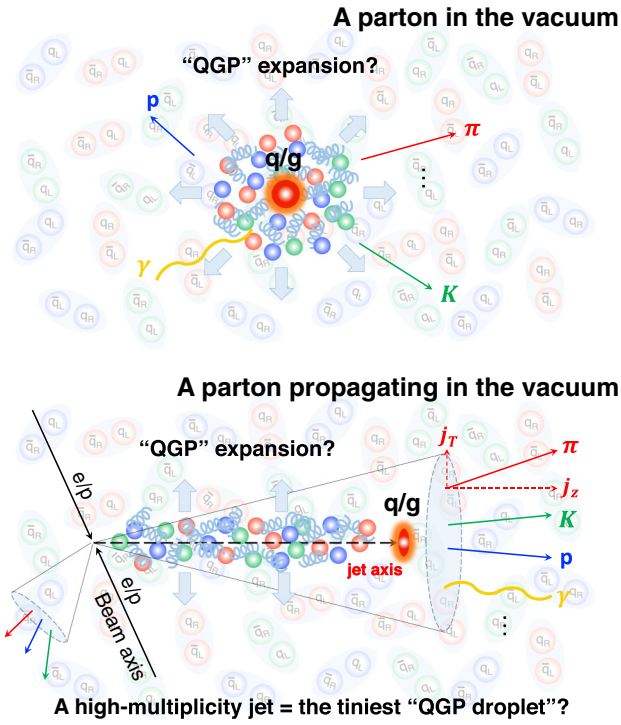

FIG. 1. Cartoons of a single parton evolving at rest in the vacuum (top) and fast-moving through the vacuum (bottom).

original isolated parton, a local, dense partonic system will be formed. Indeed, it may be possible that so many partons will be excited from the vacuum that many of them will have a significant overlap with each other in space and time, which may allow for strong rescatterings between partons. If such rescatterings occur, this may lead to a collective expansion of the partons in the system as they 'explode' away from the initial source of high energy densities. Obviously, the kind of initial conditions depicted in Fig. 1 (top) are not possible to set up experimentally, and a robust theoretical treatment of such a system is hindered by the initial assumption resulting in infinite potential energy in the color fields. Despite this, we remark that the qualitative behavior conjectured here would be strongly reminiscent of some current models of collective the evolution of a QGP liquid created in a nuclear collision.

Now let us consider more realistic scenarios, where a parton (or partons) is knocked out of a proton into the vacuum in hard scattering processes of pp collisions. In the conventional understanding of such a process, the struck parton is highly virtual and can be treated as an essentially free parton because of QCD factorization. However, it immediately begins to shed this virtuality via fragmentation into additional partons in processes that can be calculated by perturbative QCD (pQCD). For example, it is shown by Mueller in Ref. [65] that pQCD calculations can describe *energy dependence* of hadron multiplicity in e^+e^- collisions producing jets (although it cannot calculate the absolute scale of hadron multiplicity, which is nonperturbative). Once the virtuality scale approaches $\approx$1 GeV, nonperturbative effects become dominant and the system eventually hadronizes into a shower of final-state particles via inherently nonperturbative processes. Phenomenological models of hadronization, such as the Lund string model [4], are often employed to describe the remaining details of nonperturbative dynamics. There, excited QCD string systems will create $q\bar{q}$ from the strong field through Schwinger mechanism and form hadrons in the final state [4]. While the string picture is successful in characterizing many aspects of the parton fragmentation and hadronization process, it still has limitations such as its dependence on many tuning parameters, and its inability to describe the "thermal behavior" observed in e^+e^- collisions.

We can construct a thought experiment similar the one previously described for an isolated parton, but let the parton be Lorentz-boosted to a fast-moving frame, as illustrated in Fig. 1 (bottom). The scenario is evocative of a similar situation as the beginning stages of a jet's evolution. In this alternative picture, as the initial parton propagates through the vacuum, its strong color fields will similarly excite (anti)partons along its path. These excitations develop at the cost of the original parton's energy. In the case of very high-multiplicity final states, it is plausible to imagine that the created parton (or string) densities are strong enough to result in overlaps and rescattering effects, which could manifest themselves as a collective expansion. In this scenario, the expansion would be most pronounced in the direction transverse to the initial direction of the propagating parton, creating a pattern of partons which is evocative of a "jet". We should stress that a key motivation for proposing this alternative picture of a parton fragmenting is to try to capture features of non-perturbative processes which are not described by the conventional picture (unless rescattering effects are implemented). These processes may have connection to the apparent thermal behavior of hadrons in e^+e^- collisions.

In the conventional picture, the initiating parton starts with a large virtuality which monotonically decreases. However, an isolated parton propagating would start in an on-shell state and gain virtuality through the excitation of additional partons. Nonetheless, as a conventional parton shower evolves towards a collection of low-virtuality partons around the nonperturbative scale, we postulate that certain aspects of systems having many rescatterings and/or collective expansion may also be present in the nonperturbative dynamics of the jet's evolution, similar to the thought experiment previously described. If this is the case, we believe high-multiplicity jets, corresponding to a large number of produced partons—and presumably a higher probability of strong rescatterings in this nonperturbative picture—would be the best opportunity to study such behavior. Likewise, for a more dilute system of partons such as a low-multiplicity jet, we expect any rescattering effects to be small enough that existing pQCD and phenomenological models will be sufficient to describe the dynamics of the system.

Experimentally, the process of parton fragmentation into hadrons has been studied extensively at colliders. Recent studies of jet substructure [6], have offered new insights into our understanding of the parton fragmentation process, but many of the techniques developed there are based on the pQCD and tend to trim away soft-radiated particles where intriguing nonperturbative QCD phenomena may occur. Thus, our goal

in this paper is to focus on studying soft particle production with respect to the jet axis, with particular emphasis on searching for signatures of thermalization and collective expansion effects (such as radial and elliptic flow as will be discussed in detail later). We postulate that these effects are particularly likely to develop in high-multiplicity jets, where there may be the possibility of creating a system that is characterized by many rescatterings.

III. SEARCH FOR "QGP-LIKE" SIGNATURES WITHIN INDIVIDUAL JETS

The analysis strategy discussed in this paper is universally applicable to any high-energy collision system including pp, e^+e^-, and e^-p, where energetic jets (often dijets) are copiously produced. High transverse momentum (relative to the beam axis) jets are first reconstructed in an event using a particular algorithm (e.g., anti-k_t [66]) with a choice of jet cone size. For an individual jet we define a new coordinate frame such that the z axis is aligned with the direction of jet momentum, named the *jet frame*, as illustrated in Fig. 1. Momentum vectors of all particles found within the jet cone are then redefined in this new frame, $\vec{p}^* = (j_T, \eta^*, \phi^*)$. Here, j_T is the particle transverse momentum with respect to the jet axis. By selecting very high p_T jets, effects of particles from the underlying event that coincidentally fall inside the jet cone can be significantly suppressed. We then propose to study a wide range of key QGP signatures, observed in AA collisions, for particles produced inside high-p_T jets under this new frame as a function of charged multiplicity inside the jet cone, denoted as $N_{\rm ch}^j$. We use the PYTHIA 8 Monte Carlo (MC) event generator [67] to demonstrate the proposed analysis strategy.

We first investigate some basic properties of particles produced within a jet in the new frame. As an illustration of the type of events that are being selected in this analysis, a sample PYTHIA 8 dijet event of pp collisions at $\sqrt{s} = 13$ TeV is shown in Fig. 2, in the transverse plane of the laboratory frame. The display perspective is along a weak axial magnetic field, which causes the charged particles to bend in arcs. The two jets are produced and reconstructed with the anti-k_t [66] algorithm of cone size $R = 0.8$, each having p_T of roughly 900 GeV. The first jet has a fairly average multiplicity of 27, while the second jet has over 4 times as many charged particles, and would be classified as 'high multiplicity'. Different colors of particle trajectories indicate different particle species, such as pions, kaons and protons. Jets reconstructed with smaller cone sizes (e.g., $R = 0.4$) are also investigated and show qualitatively similar properties of observables studied in this paper so we focus on presenting results only for jet cone size of 0.8. The PYTHIA sample used in this study corresponds to an integrated luminosity of approximately 50 fb^{-1} and is filtered to select events having a minimum invariant transverse momentum ($\hat{p_T}$) of 470 GeV.

Figure 3 shows multiplicity distributions of charged particles within an AK8 (anti-k_t reconstruction of cone size $R = 0.8$) jet of $p_T > 500$ GeV and $p_T > 800$ GeV in PYTHIA 8. The most likely values of charged particle multiplicity are around 25 for both jet p_T selections, but the distribution for

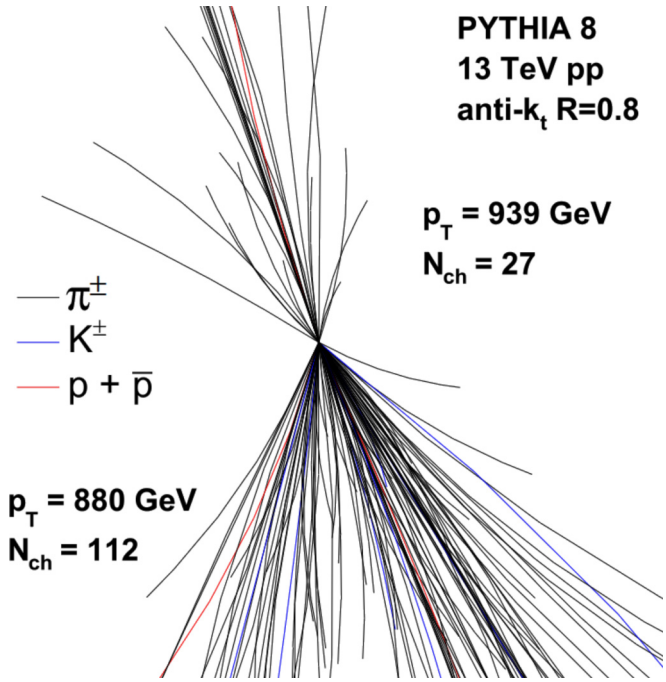

FIG. 2. A simulated event display for a PYTHIA 8 dijet event in the transverse plane with a weak axial magnetic field. One of the two jets has a high multiplicity of charged particles ($N_{\rm ch}^j$), found by the anti-k_t algorithm with a cone size of $R = 0.8$. Other particles not assigned to the two main jets by the jet finding algorithm (e.g., from the underlying event) are not shown.

higher-p_T jets has a slightly longer tail at higher multiplicities, reaching up to 140 charged particles. This can be understood as the higher jet momentum causes more produced particles to fall within the jet cone because of the larger Lorentz boost associated with the increased parton momentum. However, the difference between the two selections for a given multiplicity

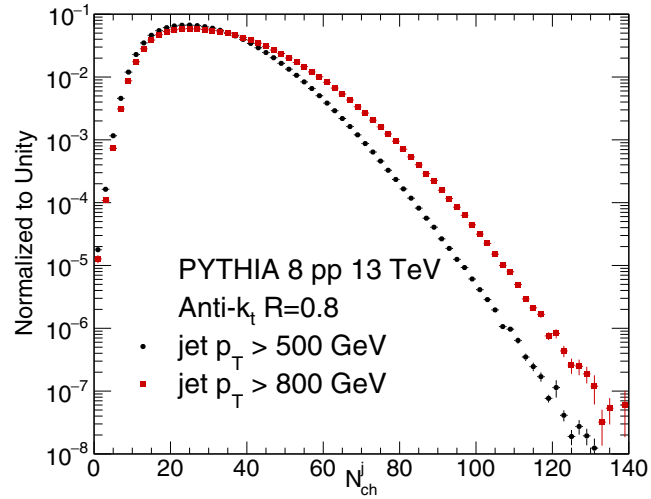

FIG. 3. Charged multiplicity distributions of jets with $p_T > 500$ GeV and 800 GeV, respectively. Jets are found by the anti-k_t algorithm with a cone size of $R = 0.8$.

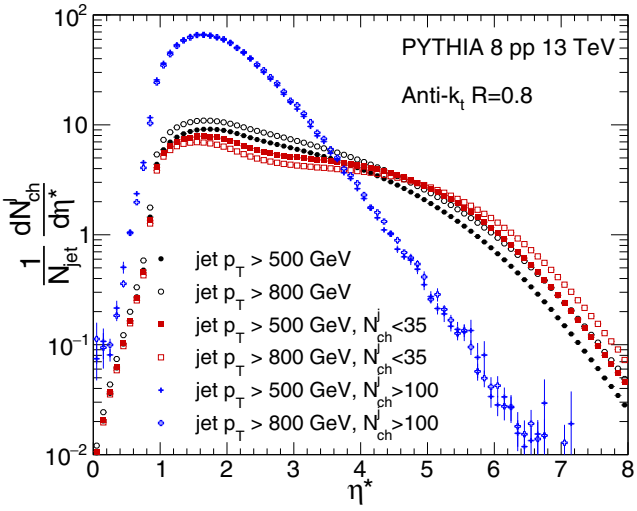

FIG. 4. The pseudorapidity (η^*) distributions of charged particle densities in the single jet frame for low ($N^j_{\rm ch} < 35$)- and high($N^j_{\rm ch} > 100$)-multiplicity jets with $p_T > 500$ GeV and 800 GeV, respectively. Jets are found by the anti-k_t algorithm with a cone size of $R = 0.8$.

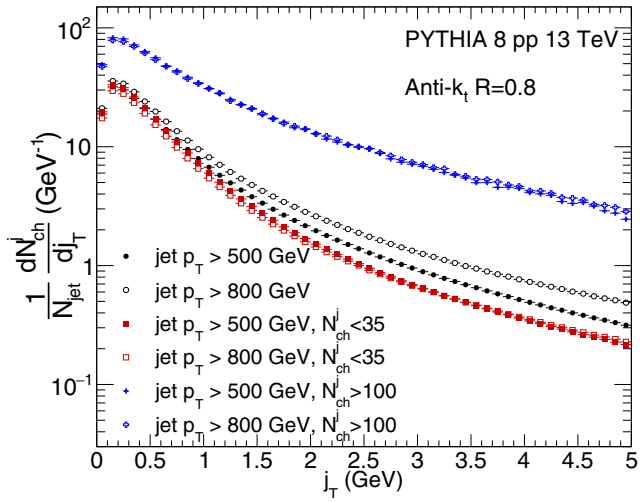

FIG. 5. The j_T distributions of charged particles in the single jet frame for low ($N^j_{\rm ch} < 35$)- and high($N^j_{\rm ch} > 100$)-multiplicity jets with $p_T > 500$ GeV and 800 GeV, respectively. Jets are found by the anti-k_t algorithm with a cone size of $R = 0.8$.

probability is only around 10 charged particles at high multiplicities, indicating only a loose correlation between jet p_T and multiplicity, which is also observed in experimental data at sufficiently high jet p_T [68]. Given that high-multiplicity jets are rarely produced and that they are only loosely correlated with jet p_T, suggested by Fig. 3, standard p_T-based experimental online triggers are not optimal for studying these systems, and a dedicated trigger filtering on high multiplicities from a single jet will significantly enhance the potential of searching for new phenomena.

Distributions of charged particle densities in pseudorapidity of the jet frame, $dN_{ch}/d\eta^*$, within an AK8 jet are shown in Fig. 4. In the jet coordinate system, low η^* corresponds to particles that are separated from the main jet axis by a large angle, while high η^* corresponds to particles more collimated with the jet direction. The closed points show distributions for jet $p_T > 500$ GeV, while open points correspond to $p_T > 800$ GeV. An inclusive multiplicity selection is shown in black, while low ($N^j_{\rm ch} < 35$) and high ($N^j_{\rm ch} > 100$) multiplicity selections are shown in red and blue, respectively.

The distribution tends to shift towards lower values of η^*, i.e., large emission angles for the high multiplicity selection, as compared to the inclusive and low multiplicity selections. A similar shift was observed when comparing gluon-initiated jets to quark-initiated jets at the same jet p_T. Thus, a potential explanation for this effect is a correlation between the multiplicity of a jet and the flavor of its initiating parton. All three selections have a very sharp rising trend around $\eta^* = 0.86$ which is related to the angle the particle makes with respect to the jet axis being near the chosen cone size of 0.8. For the high multiplicity selection, the $dN_{\rm ch}/d\eta^*$ reaches values of nearly 70, which is comparable to the multiplicity regime where collective effects have been observed in high-multiplicity pp collisions [30–33]. Therefore, it is feasible to expect that similar multiparton dynamics may be developed inside a jet of sufficiently high multiplicity. Unlike in pp and AA collisions where there is a wide plateau region in $\mathrm{d}N_{\rm ch}/\mathrm{d}\eta$ over a few units, the η^* distribution of a single jet is much narrower, especially at large multiplicities. Figure 5 shows j_T distributions of charged particle yields for two different jet p_T selections and multiplicity selections. All selections exhibit a sharp peak at low j_T values, but the tail of the low-multiplicity selection falls off slightly faster than the inclusive selection. This is consistent with particles in these jets being emitted as narrower angles relative to the jet axis on average, as was already observed in the $dN_{ch}/d\eta^*$ distribution. The distributions for the high-multiplicity selection are remarkably similar for both jet p_T choices.

In the following subsections, we employ the PYTHIA 8 generator as a baseline to investigate a series of observables relevant to signatures of a QGP and explore potential discoveries in future experiments. No effects of rescatterings among produced parton showers or strings are expected for the parton fragmentation process in PYTHIA 8 (or any other MC event generator presently on the market). The list of observables is not exhaustive but rather representative of key signatures:

(i) Particle multiplicity and *strangeness enhancement* in a dense, thermal partonic medium;
(ii) Long-range correlations and *anisotropy flow*;
(iii) *Radial flow* boost to identified particle j_T spectra;
(iv) *Quantum Interference* of identical particles.

We shall emphasize that while the ultimate goal is to implement rescattering (or "QGP") effects to the modeling of the parton fragmentation process to make quantitative predictions of data, we intend to leave that for future work where dedicated phenomenological efforts and likely some guidance from experimental data are needed.

A. Particle multiplicity and strangeness enhancement

We propose to study the total multiplicity of each particle species and their relative ratios for particles produced from

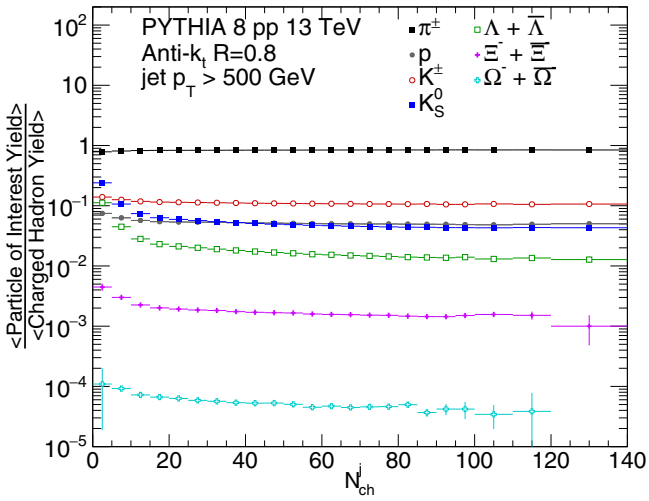

FIG. 6. Ratios of total yields of various hadrons to inclusive charged hadrons from AK8 jets for jet $p_T > 500$ GeV, as a function of charged multiplicity in jet ($N^j_{\rm ch}$), in PYTHIA 8 pp events at $\sqrt{s} = 13$ TeV.

a single jet in a similar fashion to those in other collision systems. Statistical models can also be used to describe the particle multiplicity data in jets to search for evidence of thermal production from a fragmenting parton that may be related to the quantum entanglement effect or a strongly interacting medium. In the analysis presented here, we specifically focus on the aspect of strange hadron multiplicities and explore possible strangeness enhancement phenomena as a function of the charged multiplicity in jets, using the PYTHIA 8 model.

The enhancement of strange hadron production (relative to nonstrange hadrons) in AA collisions has been considered as strong evidence for the existence of a high-gluon density QGP medium, where the gluon splitting channel dominates the strangeness production [69]. In recent years, it has also been observed that in small pp and pA systems, strange hadron yields relative to pions smoothly increase as higher multiplicity events are selected [70] toward multiplicity values in AA collisions. The PYTHIA 8 model is unable to reproduce the observed strangeness enhancement in pp collisions.

We propose to explore similar strangeness enhancement phenomena in high p_T jets, as a function of jet multiplicity. Using PYTHIA 8 as a reference, the markers in Fig. 6 show the ratio of various light and strange hadron yields in a high-p_T (>500 GeV) AK8 jet to those of charged hadrons, as a function of the charged multiplicity of a jet ($N^j_{\rm ch}$). As expected, no strangeness enhancement is observed in PYTHIA 8. The ratios of protons to pions is nearly constant as a function of $N^j_{\rm ch}$. For strange hadrons such as kaons, Λ, Ξ^-, and Ω^-, a slight downward trend is observed for $N^j_{\rm ch}$ values less than 20, but the ratio is nearly independent of multiplicity above this threshold. Observation of an increasing strange particle-to-pion yield ratio experimentally in high-multiplicity jets would be a compelling indication of additional physics not captured by the canonical fragmentation and/or hadronization model via string breaking, but possibly involving dynamics of dense gluon interactions such as those in high-multiplicity pp, pA, and AA collisions.

B. Long-range correlations and anisotropic flow

Long-range collective phenomena over a wide pseudorapidity range have been observed in azimuthal correlations of particles from a variety of collision systems and experiments. In particular, the persistence of these collective phenomena in increasingly small systems has lead to debates about the origin of such behavior and the development of new experiments to push the limits of hydrodynamic validity and explore possible effects of quantum entanglement. We briefly describe the analytical steps of two-particle angular correlation analyses in the jet frame and discuss key features of the result. The procedure is similar to that employed in Ref. [36], except that the momentum vector of all particles are redefined in the jet frame. The two-dimensional (2D) angular correlation function is calculated as follows:

$$\frac{1}{N^{\rm trg}_{\rm ch}}\frac{d^2N^{\rm pair}}{d\Delta\eta^* d\Delta\phi^*} = B(0,0)\frac{S(\Delta\eta^*,\Delta\phi^*)}{B(\Delta\eta^*,\Delta\phi^*)}, \tag{1}$$

where $\Delta\eta^*$ and $\Delta\phi^*$ are relative pseudorapidity and azimuthal angle in the jet frame, for a pair of trigger and associate particles. The trigger and associate particles can be selected from the same or different j_T ranges. For analyses presented below, trigger and associate particles are chosen from the same j_T range for simplicity. The correlation functions are typically measured in different j_T and multiplicity ranges.

The $S(\Delta\eta^*,\Delta\phi^*)$ and $B(\Delta\eta^*,\Delta\phi^*)$ represent the signal and background distributions, respectively,

$$S(\Delta\eta^*,\Delta\phi^*) = \frac{1}{N^{\rm trg}_{\rm ch}}\frac{d^2N^{\rm sig}}{d\Delta\eta^* d\Delta\phi^*} \tag{2}$$

and

$$B(\Delta\eta^*,\Delta\phi^*) = \frac{1}{N^{\rm trg}_{\rm ch}}\frac{d^2N^{\rm bkg}}{d\Delta\eta^* d\Delta\phi^*}. \tag{3}$$

The signal distribution is calculated with pairs taken from each jet ($N^{\rm sig}$) and then averaged over all jets, weighted by the jet multiplicity. The background distribution serves as a reference and a correction to the pair acceptance due to limited η^* range. To construct the background distribution, we first derive the 2D single-particle η^*-ϕ^* distribution for daughters of all jets. Pseudoparticles are then randomly drawn from the η^*-ϕ^* distribution. These pseudoparticles are built from values accumulated over multiple distinct jets in multiple distinct events. In this way, no correlations should exist in the background distribution and all features are detector related. A large number of pseudoparticles $n_{\rm pseudo}$ are created such that $N_{\rm bkg} = n_{\rm pseudo}(n_{\rm pseudo}-1)/2 \approx 10 \times N_{\rm sig}$, where $N_{\rm sig}$ is the total number of entries in the complete signal distribution for the class. The $B(0,0)/B(\Delta\eta^*,\Delta\phi^*)$ term is the appropriate bin-by-bin correction to the signal distribution.

Figure 7 shows the 2D two-particle angular correlation function for low- and high-multiplicity jets and particles with $0.3 < j_T < 3$ GeV in PYTHIA 8 pp collisions at 13 TeV. The central peak at $(\Delta\eta^*,\Delta\phi^*) = (0,0)$ is the result of short-range correlations from local parton shower

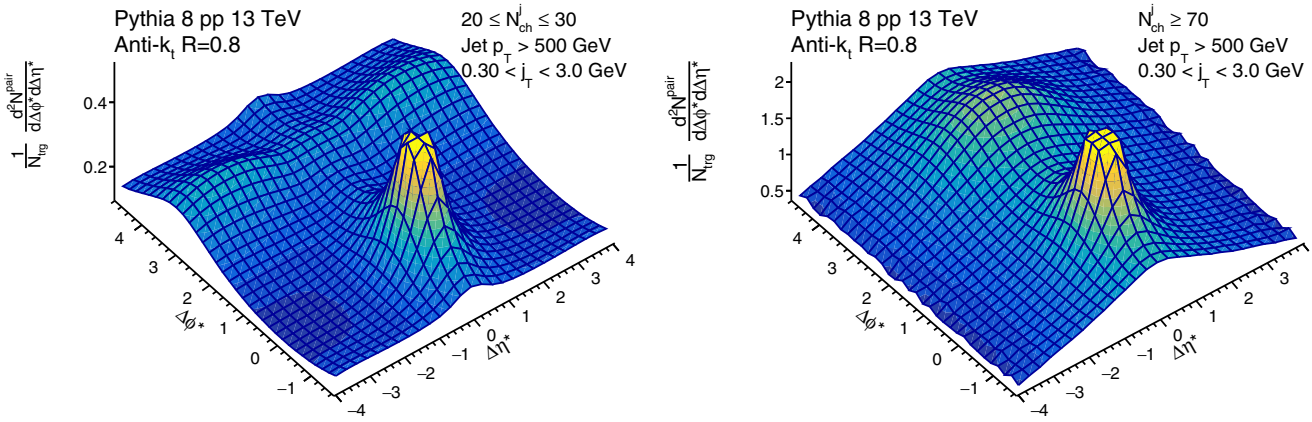

FIG. 7. The 2D two-particle angular correlation functions for particle $0.3 < j_T < 3$ GeV in low ($20 \leqslant N^j_{\rm ch} \leqslant 30$, left) and high ($N^j_{\rm ch} \geqslant 70$, right) in-jet charged multiplicity classes, for AK8 jets with jet $p_T > 500$ GeV in PYTHIA 8 pp events at $\sqrt{s} = 13$ TeV.

and hadronization. The far-side ridge at $\Delta\eta^* \approx \pi$ is mostly related back-to-back particle production by conservation of momentum. These prominent features have been found in laboratory-frame analyses for both experimental data and MC simulations. Moreover, another feature commonly observed in AA collisions is the near-side enhancement at $\Delta\phi^* \approx 0$ over long-range in $\Delta\eta^*$, commonly known as the near-side "ridge". The persistence of this ridge to very small systems, such as pp and pA collisions, naturally motivates a proposal to continue searching for these effects in even smaller systems, like a single jet. As expected, there is no indication of a near-side ridge for both low- and high-multiplicity jets in PYTHIA 8. This is also consistent with e^+e^- [63] and e^-p collisions [64] at relatively low final-state multiplicity.

The resulting 2D distribution can be further understood by decomposition into a one-dimensional (1D) Fourier series of projections along the $\Delta\phi^*$ axis:

$$\frac{1}{N^j_{\rm ch}}\frac{dN^{\rm pair}}{d\Delta\phi^*} \propto 1 + 2\sum_{n=1}^{\infty} V_{n\Delta}\left(j_T^A,\, j_T^B\right)\cos(n\Delta\phi^*), \qquad (4)$$

where j_T^A and j_T^B represent the j_T of trigger and associate particles, respectively. By taking 1D $\Delta\phi^*$ projections over $\Delta\eta^* > 2$, we exclude the short-range correlations and focus on understanding structure with large pseudorapidity separations. The strength of the Fourier components in such decomposition can give indications of the type of flow and its relative significance in various systems. The second Fourier component is typically associated with the strength of elliptical flow while the third is associated with the triangular flow.

In Fig. 8, 1D $\Delta\phi^*$ correlation functions for $|\Delta\eta^*| > 2$ are shown for $20 \leqslant N^j_{\rm ch} \leqslant 30$ and $N^j_{\rm ch} \geqslant 70$, respectively, for particles with $0.3 < j_T < 3$ GeV from AK8 jets in PYTHIA 8 pp collisions at 13 TeV. For both multiplicity classes, strong away-side correlations are observed, consistent with dominant contributions of momentum conservation. The near-side at $\Delta\phi^* \approx 0$ shows a minimum, although there seems to be an indication of a slight enhancement for $N^j_{\rm ch} \geqslant 70$. That enhancement is not significant and may also be related to the tail of short-range correlations at very large $\Delta\eta^*$.

The markers and solid lines in Fig. 9 show the extracted two-particle Fourier coefficients, $V_{n\Delta}$, as a function of the charged multiplicity in jet ($N^j_{\rm ch}$), for the first three harmonic components, from AK8 jets in PYTHIA 8 pp collisions at 13 TeV. Over the full $N^j_{\rm ch}$ range, the odd-order harmonics, $V_{1\Delta}$ and $V_{3\Delta}$, are negative, while the even-odd harmonics, $V_{2\Delta}$ are positive. Magnitudes of all harmonics decrease as $N^j_{\rm ch}$ increases. All these features are consistent with expectation of short-range back-to-back correlations that are not related to collective effects. The contribution of short-range few-body correlation to the global azimuthal anisotropy of the event generally diminishes as $1/N^j_{\rm ch}$ in the two-particle Fourier coefficients. An increase of $V_{2\Delta}$ or a significant positive $V_{3\Delta}$ signal at very high multiplicity could be an indication of the onset of collective flow effects in the expansion of the parton jet. Note that the single-particle azimuthal anisotropy Fourier coefficient, v_n, is related to the two-particle Fourier coefficient as $V_{n\Delta}(j_T^A, j_T^B) = v_n(j_T^A)v_n(j_T^B)$. Pink dashed lines in Fig. 9 indicate values of $V_{2\Delta}$ equivalent to 5%, 10%, and 15% in single particle v_2. Therefore, if PYTHIA 8 properly models short-range correlations in the parton fragmentation process, an additional 15% v_2 enhancement should be clearly identifiable with jets of $N^j_{\rm ch} > 70$, while a much smaller v_2 enhancement of 5% would require pushing to much higher multiplicity jets, such as $N^j_{\rm ch} > 90$–100.

C. Identified particle j_T spectra and radial flow

The hydrodynamic expansion of the QGP will generate a common velocity field that collectively boosts all produced particles along the radial expansion direction. This phenomenon is known as the "radial flow" (see a review in Ref. [28]). As a consequence, final-state particles receive a push to higher average transverse momentum with heavier particles gaining more momentum, proportional to the mass. This effect can be observed and quantified by measuring the average p_T of various particle species in a collision. Besides the average p_T, the average transverse kinetic energy, $KE_T \equiv m_T - m = \sqrt{p_T^2 + m^2} - m$, is also often used and has the advantage of unifying particle species of different masses

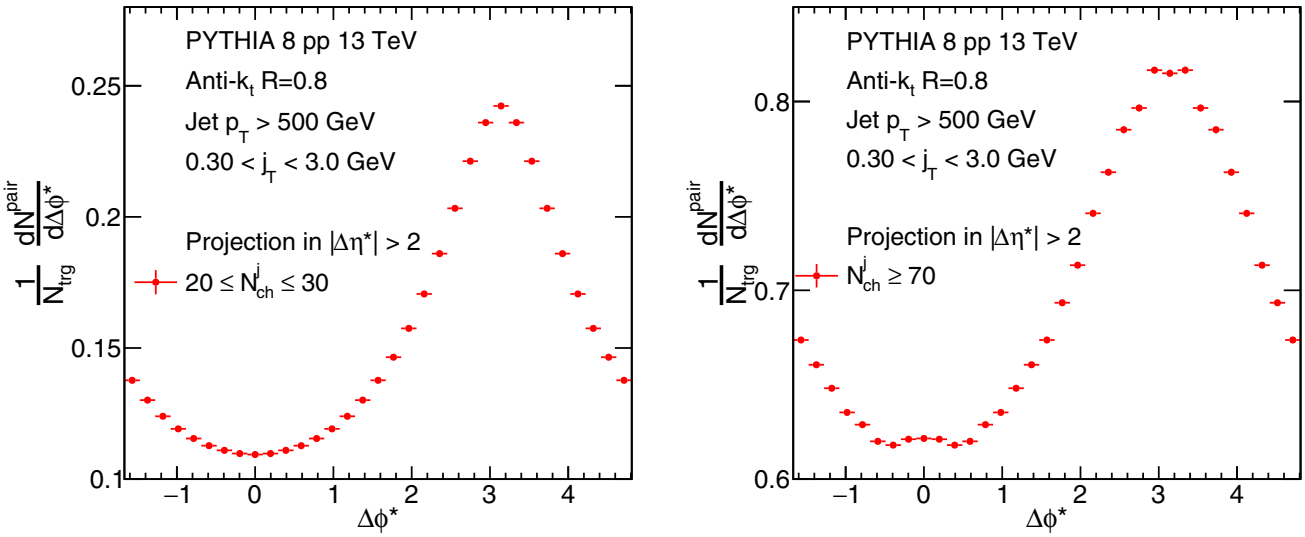

FIG. 8. The 1D $\Delta\phi^*$ two-particle angular correlation functions for particle $0.3 < j_T < 3$ GeV and $|\Delta\eta^*| > 2$, in low ($20 \leqslant N^j_{\rm ch} \leqslant 30$, left) and high ($N^j_{\rm ch} \geqslant 70$, right) in-jet charged multiplicity classes, for anti-k_t $R = 0.8$ jets with jet $p_T > 500$ GeV in PYTHIA 8 pp events at $\sqrt{s} = 13$ TeV.

(known as the "m_T scaling" [71]) in absence of the radial flow. The m_T scaling of hadron production in high-energy collisions was proposed as early as 1965 by Hagedorn based on a statistical thermodynamic approach [72]. It has been observed in minimum bias pp collisions, indicating negligible radial flow effects. In high energy AA and also high-multiplicity small systems, significant breaking of m_T scaling is observed as the multiplicity or system size increases [12,14,73–75].

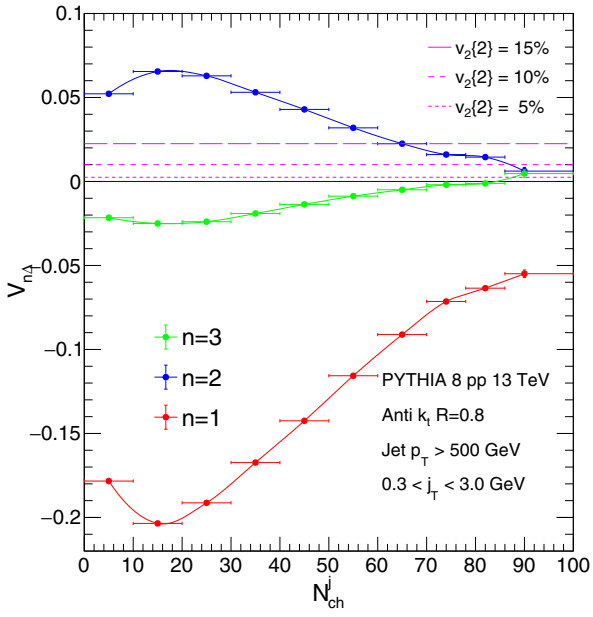

FIG. 9. The extracted two-particle Fourier coefficients, $V_{n\Delta}$, as a function of the charged multiplicity in jet ($N^j_{\rm ch}$), for the first three harmonic components, from AK8 jets in PYTHIA 8 pp collisions at 13 TeV. The dashed lines indicate values of $V_{2\Delta}$ equivalent to 5%, 10%, and 15% in single particle v_2.

We present the average kinetic energy, $\langle m^*_T \rangle - m$, calculated in the jet frame in Fig. 10, for inclusive charged hadrons, charged pions, charged kaons, protons, K^0_s, Λ, Ξ^-, and Ω^- produced within AK8 jets, for jet $p_T > 500$ GeV as a function of charged multiplicity in jet ($N^j_{\rm ch}$) in PYTHIA 8 pp events at $\sqrt{s} = 13$ TeV. The m_T scaling is indeed present for low-multiplicity jets ($N^j_{\rm ch} < 10$) in PYTHIA 8. As $N^j_{\rm ch}$ increases, an increasing trend of $\langle m^*_T \rangle - m$ is observed for all particle species but they do not appear to fall on a common trend. Instead, heavier particles appear to have greater average kinetic energy values, and by extension, greater average j_T values as well. This trend is qualitatively similar to that observed

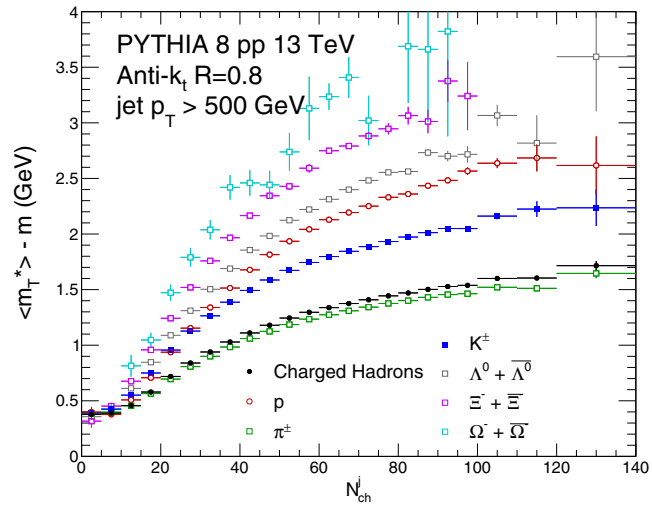

FIG. 10. The average transverse kinetic energy of various particle species produced from AK8 jets for jet $p_T > 500$ GeV, as a function of charged multiplicity in jet ($N^j_{\rm ch}$), in PYTHIA 8 pp events at $\sqrt{s} = 13$ TeV.

in high-multiplicity *pp*, *pA*, and *AA* collisions. The rate of increase of m_T with multiplicity seems greatest in the range of $N_{\rm ch}^{j} \approx 20$–$30$, with a flattening trend at higher multiplicities. The breakdown of m_T scaling as a function of multiplicity in PYTHIA 8 is possibly related to the color reconnection effect, which effectively generates a boost to final-state particles. Therefore, this observable alone should not be taken as a unique signature of the QGP-like state formation. Quantitative comparison with theoretical calculations, as well as supporting evidence from other observables, would be necessary to draw a conclusion.

D. Quantum interference of identical particles

The Bose-Einstein correlations (BEC), or interferometry exploits quantum interference effects of identical particles produced with overlapping wave functions in phase space. By studying momentum correlations of two identical bosons (fermions), an enhancement (depletion) will be observed at small momentum difference between two particles. The size of the source of particle emission at "freeze-out" (when particles cease to interact) in spacial coordinate space can then be inferred from the correlation range in the momentum space. The two-particle intensity interferometry method was first invented by Hanbury Brown and Twiss (HBT) to measure the size of astronomical objects [76]. It has since been extensively applied to extract the space-time structure of QGP in *AA* collisions [77–79].

In this study, the two-particle BEC correlation function is defined as the ratio

$$C_2(\vec{q}^{\,*}) \equiv \frac{S(\vec{q}^{\,*})}{B(\vec{q}^{\,*})}, \tag{5}$$

where $\vec{q}^{\,*} = \vec{p}_1^{\,*} - \vec{p}_2^{\,*}$ is the momentum difference between the two particles in the jet frame. Similar to two-particle angular correlations, the $S(\vec{q}^{\,*})$ is the measured particle pair distribution from the same jet containing potential BEC signals, while the $B(\vec{q}^{\,*})$ is formed with pairs of random pseudoparticles as a reference, as well as for correction of detector effects. The BEC studies can be performed in one, two or three dimensions of $\vec{q}^{\,*}$. For simplicity, we present a 1D analysis in $q_{\rm inv}^{*} = |\vec{q}^{\,*}|$ using charged pions from jets in PYTHIA 8 as a function of the charged multiplicity in jet ($N_{\rm ch}^{j}$) and pair transverse momentum, $k_T^{*} = \frac{1}{2}|\vec{j}_{T,1} + \vec{j}_{T,2}|$, to demonstrate the idea. No BEC signals are implemented in the PYTHIA 8 MC generator.

Figure 11 presents 1D BEC correlation functions for pairs of same-sign charged pions in $q_{\rm inv}^{*}$ in different $N_{\rm ch}^{j}$ ranges of AK8 jets in PYTHIA 8 *pp* events at $\sqrt{s} = 13$ TeV. Each panel of Fig. 11 shows results for each k_T^{*} range.

All $C_2(\vec{q}^{\,*})$ distributions show a general trend of enhanced correlations toward $q_{\rm inv}^{*} \approx 0$. This feature is qualitatively similar to those observed in *AA* collisions [79], where quantum interference effects are believed to play the dominant role. The width of $C_2(\vec{q}^{\,*})$ is inversely proportional to the size of the particle-emitting source. As mentioned earlier, there are no BEC correlations expected in PYTHIA 8. Therefore, these results reflect the background contributions from the fragmentation. To distinguish the background contribution from true

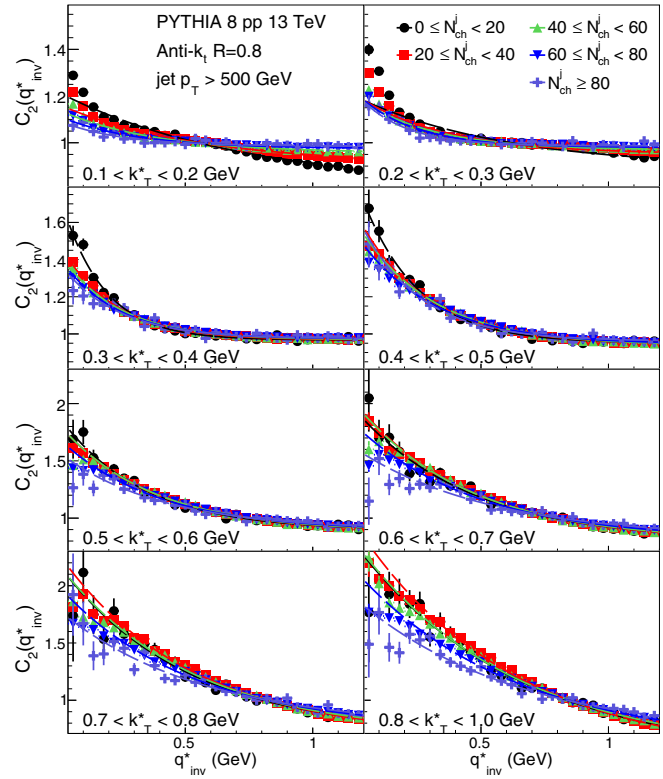

FIG. 11. The 1D BEC correlation functions for pairs of same-sign charged pions in several ranges of charged multiplicity in jet, $N_{\rm ch}^{j}$, for AK8 jets with jet $p_T > 500$ GeV in PYTHIA 8 *pp* events at $\sqrt{s} = 13$ TeV. Each panel represents a range of pair transverse momentum k_T^{*}, defined in the single jet frame.

BEC signals, it is necessary to investigate the detailed $N_{\rm ch}^{j}$ and k_T^{*} dependence.

The 1D BEC correlation function is fitted by an exponential function

$$C\left(1 + \lambda e^{-R_{\rm inv}^{*} q_{\rm inv}^{*}}\right), \tag{6}$$

where the parameter, $R_{\rm inv}^{*}$, characterizes the size of the coherent source (in unit of fm). The extracted values of $R_{\rm inv}^{*}$ are shown in Fig. 12, as a function of k_T^{*}, for several $N_{\rm ch}^{j}$ ranges of AK8 jets $p_T > 500$ GeV in PYTHIA 8 *pp* events at $\sqrt{s} = 13$ TeV.

In *pp*, *pA*, and *AA* collisions, the BEC radii parameter is observed to monotonically increase as the pair momentum decreases. This can be understood by the uncertainty principle that larger sources tend to coherently emit particles at lower momenta. The BEC radii are also found to increase with event multiplicity approximately to the power of $1/3$, which is again consistent with the formation of a medium that expands collectively. In the BEC analysis of particles in the jet frame using PYTHIA, shown in Fig. 12, similar features of extracted radii in *AA* collisions are not observed. As seen in Fig. 12, the radii parameter in the jet frame, $R_{\rm inv}^{*}$, shows a nonmonotonic behavior as a function of k_T^{*}, which first increases but then decreases toward low k_T^{*}. While the $R_{\rm inv}^{*}$ does increase with $N_{\rm ch}^{j}$ for $k_T^{*} < 0.3$ GeV, this trends becomes opposite at higher

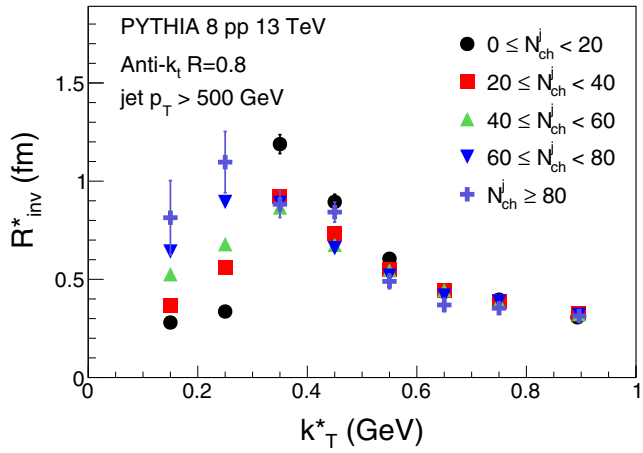

FIG. 12. The extracted 1D BEC radii for charged pions as a function of pair transverse momentum k_T^*, defined in the single jet frame, in several ranges of charged multiplicity in jet, $N_{\rm ch}^j$, for AK8 jets with jet $p_T > 500$ GeV in PYTHIA 8 pp events at $\sqrt{s} = 13$ TeV.

k_T^*. Therefore, a systematic study of BECs for particles in high-p_T jets as a function of multiplicity and pair transverse momentum in the jet frame has the potential to provide key evidence for the formation of a system with extended space-time structures.

IV. DISCUSSIONS

In this paper, we have been focusing on studies of particles produced in inclusive single jets with high multiplicity in pp collisions at LHC energies. There are many possible extensions of proposed analyses in other directions to explore new phenomena in high density QCD physics experimentally. We discuss a few examples below.

Thermal photon emission: In AA collisions, the observation of a large excess of soft photons at low p_T (<1 GeV) over the primordial hard photon production in perturbative QCD processes [80–82] is considered as direct evidence for the formation of a thermalized QGP medium. The slope of excess photon p_T spectra provides direct information of the QGP's temperature. If such a medium was produced in a high-multiplicity jet system, a similar enhancement of photons at small j_T inside the jet cone would also be expected. Those photons are typically identified as fragmentation photons, emitted from parton showers. Even if emitted with small j_T, these photons could still have a relatively large p_T in the laboratory reference frame, and therefore be measured by experiments like CMS and ATLAS, which have calorimeters optimized for the high-p_T photon regime. However, this type of measurement will have to deal with huge backgrounds originating from hadron (e.g., π^0) decays, as well as underlying event contributions and will be undoubtedly extremely challenging. At high energy lepton-lepton and lepton-hadron collisions, the the underlying event background is much cleaner. Therefore, future high-energy e^+e^- colliders and the electron-ion collider planned in the USA may provide an ideal environment to search for thermal photon production from a single parton.

Dijets and vector boson-jet systems: Vector boson-jet events, such as Z/γ jets, in pp collisions are ideal tools to study quark propagation in the vacuum and possible collective effects developed around the quark direction of motion. All analyses performed with inclusive jets can be done with Z/γ jets in the same way. A back-to-back dijet system in pp collisions is reminiscent of the final state of e^+e^- collisions, where a color string may be stretched between the two fast-moving partons and develop interesting dynamics. Correlating particles from two different jets also helps extend the rapidity gap of two particles and benefit the search for long-range correlations. There are some complications to analyses in the dijet system though. As the two jets are never exactly back to back, choosing a common z axis for the new frame (e.g., the thrust axis) may lead to some smearing if the proposed collective effects are strongest with respect to each individual jet direction. This is particularly an issue, when a hard third jet is present. More careful studies would be needed.

Winner-take-all jet recombination: As the first step of all proposed analyses is to rotate the laboratory frame to a new frame where the jet direction represents the beam axis, the choice of the jet axis (which is not unique) plays a crucial role. Besides the standard "E-scheme" recombination [66] of jet reconstruction, where the jet axis and the jet momentum are aligned at each stage of the recursion, the "winner-take-all" scheme [83,84] chooses the jet axis to be align with the harder particle in a pair-wise recombination. The motivation of the winner-take-all scheme is to minimize the impact of soft radiation recoils to the initial parton direction. It would be interesting to investigate how all observables would depend on different choices of jet axis.

Lepton-lepton or lepton-proton/ion collisions: As all proposed studies take place within a single jet, they are in principle independent of the initial colliding beam species, which can be protons, leptons or ions. Therefore, these studies are highly relevant not only to the LHC but also all future high-energy colliders. In fact, e^+e^- or e^-p colliders may even provide a cleaner environment for studying high-multiplicity jets, as the underlying event contribution is much smaller.

Jets in heavy ion collisions: Finally, the study of parton energy loss in a QGP medium has been a main theme of research in AA collisions. In our thought experiment, a parton propagating in the vacuum or the QGP has no fundamental difference. In both cases, the parton loses its energy by interacting with other partons along its passage. The only difference is that in the QGP medium, surrounding partons are excited and thus have stronger color fields, which lead to larger energy loss than interactions with vacuum chiral condensates. Doing the same analyses for jets in heavy ion collisions may provide insights to develop a unified approach to describing parton energy loss in confined and deconfined environments.

V. SUMMARY

Motivated by early surprises of thermal and collective phenomena in small system collisions, we postulate that non-perturbative QCD evolution of a fragmenting parton in the

vacuum will develop similar long-range collective effects to those of a multiparton system, reminiscent of what is observed in high-energy hadronic or nuclear interactions with high-multiplicity final-state particles. We propose searches for these properties of a parton propagating in the vacuum using high-p_T jets produced with large multiplicities in high-energy elementary collisions, e.g., at the LHC. A set of key observables are studied in detail using the PYTHIA 8 Monte Carlo event generator, where no collective or QGP effects are expected inside the jet. Experimental observation of the proposed effects (e.g., long-range collectivity or strangeness enhancement) in a single jet will offer a new view of non-perturbative QCD dynamics of multiparton systems at the smallest scales. On the other hand, absence of these effects may offer new insights in to the role of quantum entanglement in the observed thermal behavior of particle production in high energy collisions.

ACKNOWLEDGMENTS

The authors would like to thank Jamie Nagle, Zhoudunming Tu, and Raju Venugopalan for useful discussions. This work is in part supported by the Department of Energy under Grant No. DE-SC0005131.

[1] D. J. Gross and F. Wilczek, Ultraviolet Behavior of Non-Abelian Gauge Theories, Phys. Rev. Lett. **30**, 1343 (1973).
[2] H. Politzer, Reliable Perturbative Results for Strong Interactions?, Phys. Rev. Lett. **30**, 1346 (1973).
[3] R. Brock *et al.* (CTEQ Collaboration), Handbook of perturbative QCD: Version 1.0, Rev. Mod. Phys. **67**, 157 (1995).
[4] B. Andersson, G. Gustafson, G. Ingelman, and T. Sjostrand, Parton fragmentation and string dynamics, Phys. Rep. **97**, 31 (1983).
[5] G. Marchesini, B. Webber, G. Abbiendi, I. Knowles, M. Seymour, and L. Stanco, HERWIG: A Monte Carlo event generator for simulating hadron emission reactions with interfering gluons. Version 5.1 - April 1991, Comput. Phys. Commun. **67**, 465 (1992).
[6] R. Kogler *et al.*, Jet substructure at the Large Hadron Collider: Experimental review, Rev. Mod. Phys. **91**, 045003 (2019).
[7] F. Karsch, The Phase transition to the quark gluon plasma: Recent results from lattice calculations, Nucl. Phys. A **590**, 367 (1995).
[8] F. Karsch, Lattice QCD at high temperature and density, Lect. Notes Phys. **583**, 209 (2002).
[9] A. Bazavov *et al.* (HotQCD Collaboration), Chiral crossover in QCD at zero and non-zero chemical potentials, Phys. Lett. B **795**, 15 (2019).
[10] CERN press release 10 Feb.2020.
[11] I. Arsene *et al.* (BRAHMS Collaboration), Quark gluon plasma and color glass condensate at RHIC? The perspective from the BRAHMS experiment, Nucl. Phys. A **757**, 1 (2005).
[12] K. Adcox *et al.* (PHENIX Collaboration), Formation of dense partonic matter in relativistic nucleus-nucleus collisions at RHIC: Experimental evaluation by the PHENIX collaboration, Nucl. Phys. A **757**, 184 (2005).
[13] B. B. Back *et al.* (PHOBOS Collaboration), The PHOBOS perspective on discoveries at RHIC, Nucl. Phys. A **757**, 28 (2005).
[14] J. Adams *et al.* (STAR Collaboration), Experimental and theoretical challenges in the search for the quark gluon plasma: The STAR Collaboration's critical assessment of the evidence from RHIC collisions, Nucl. Phys. A **757**, 102 (2005).
[15] B. Müller, J. Schukraft, and B. Wyslouch, First results from Pb+Pb collisions at the LHC, Annu. Rev. Nucl. Part. Sci. **62**, 361 (2012).
[16] J. Adams *et al.* (STAR Collaboration), Distributions of Charged Hadrons Associated with High Transverse Momentum Particles in pp and Au + Au Collisions at $\sqrt{s_{NN}} = 200$ GeV, Phys. Rev. Lett. **95**, 152301 (2005).
[17] B. Alver *et al.* (PHOBOS Collaboration), System size dependence of cluster properties from two- particle angular correlations in Cu + Cu and Au + Au collisions at $\sqrt{s_{NN}} = 200$ GeV, Phys. Rev. C **81**, 024904 (2010).
[18] B. Abelev *et al.* (STAR Collaboration), Long range rapidity correlations and jet production in high energy nuclear collisions, Phys. Rev. C **80**, 064912 (2009).
[19] B. Alver *et al.* (PHOBOS Collaboration), High Transverse Momentum Triggered Correlations over a Large Pseudorapidity Acceptance in Au + Au Collisions at $\sqrt{s_{NN}} = 200$ GeV, Phys. Rev. Lett. **104**, 062301 (2010).
[20] S. Chatrchyan *et al.* (CMS Collaboration), Long-range and short-range dihadron angular correlations in central PbPb collisions at a nucleon-nucleon center of mass energy of 2.76 TeV, J. High Energy Phys. 07 (2011) 076.
[21] S. Chatrchyan *et al.* (CMS Collaboration), Centrality dependence of dihadron correlations and azimuthal anisotropy harmonics in PbPb collisions at $\sqrt{s_{NN}} = 2.76$ TeV, Eur. Phys. J. C **72**, 10052 (2012).
[22] K. Aamodt *et al.* (ALICE Collaboration), Elliptic Flow of Charged Particles in Pb-Pb Collisions at 2.76 TeV, Phys. Rev. Lett. **105**, 252302 (2010).
[23] G. Aad *et al.* (ATLAS Collaboration), Measurement of the azimuthal anisotropy for charged particle production in $\sqrt{s_{NN}} = 2.76$ TeVlead-lead collisions with the ATLAS detector, Phys. Rev. C **86**, 014907 (2012).
[24] S. Chatrchyan *et al.* (CMS Collaboration), Studies of azimuthal dihadron correlations in ultra-central PbPb collisions at $\sqrt{s_{NN}} = 2.76$ TeV, J. High Energy Phys. 02 (2014) 088.
[25] J.-Y. Ollitrault, Anisotropy as a signature of transverse collective flow, Phys. Rev. D **46**, 229 (1992).
[26] D. Teaney, The effects of viscosity on spectra, elliptic flow, and HBT radii, Phys. Rev. C **68**, 034913 (2003).
[27] P. Romatschke and U. Romatschke, Viscosity Information from Relativistic Nuclear Collisions: How Perfect is the Fluid Observed at RHIC? Phys. Rev. Lett. **99**, 172301 (2007).
[28] U. Heinz and R. Snellings, Collective flow and viscosity in relativistic heavy-ion collisions, Annu. Rev. Nucl. Part. Sci. **63**, 123 (2013).
[29] C. Gale, S. Jeon, and B. Schenke, Hydrodynamic modeling of heavy-ion collisions, Int. J. Mod. Phys. A **28**, 1340011 (2013).

[30] V. Khachatryan *et al.* (CMS Collaboration), Observation of long-range near-side angular correlations in proton-proton collisions at the LHC, J. High Energy Phys. 09 (2010) 091.

[31] G. Aad *et al.* (ATLAS Collaboration), Observation of Long-Range Elliptic Azimuthal Anisotropies in $\sqrt{s} = 13$ and 2.76 TeV pp Collisions with the ATLAS Detector, Phys. Rev. Lett. **116**, 172301 (2016).

[32] V. Khachatryan *et al.* (CMS Collaboration), Measurement of Long-Range Near-Side Two-Particle Angular Correlations in pp Collisions at $\sqrt{s} = 13$ TeV, Phys. Rev. Lett. **116**, 172302 (2016).

[33] V. Khachatryan *et al.* (CMS Collaboration), Evidence for collectivity in pp collisions at the LHC, Phys. Lett. B **765**, 193 (2017).

[34] G. Aad *et al.* (ATLAS Collaboration), Measurement of Azimuthal Anisotropy of Muons from Charm and Bottom Hadrons in pp Collisions at $\sqrt{s} = 13$ TeV with the ATLAS detector, Phys. Rev. Lett. **124**, 082301 (2020).

[35] W. Li, Observation of a 'Ridge' correlation structure in high multiplicity proton-proton collisions: A brief review, Mod. Phys. Lett. A **27**, 1230018 (2012).

[36] S. Chatrchyan *et al.* (CMS Collaboration), Observation of long-range near-side angular correlations in proton-lead collisions at the LHC, Phys. Lett. B **718**, 795 (2013).

[37] B. Abelev *et al.* (ALICE Collaboration), Long-range angular correlations on the near and away side in pPb collisions at $\sqrt{s_{\rm NN}} = 5.02$ TeV, Phys. Lett. B **719**, 29 (2013).

[38] G. Aad *et al.* (ATLAS Collaboration), Observation of Associated Near-Side and Away-Side Long-Range Correlations in $\sqrt{s_{NN}} = 5.02 TeV$ Proton-Lead Collisions with the ATLAS Detector, Phys. Rev. Lett. **110**, 182302 (2013).

[39] R. Aaij *et al.* (LHCb Collaboration), Measurements of long-range near-side angular correlations in $\sqrt{s_{\rm NN}} = 5$ TeV proton-lead collisions in the forward region, Phys. Lett. B **762**, 473 (2016).

[40] B. B. Abelev *et al.* (ALICE Collaboration), Long-range angular correlations of pi, K and p in p–Pb collisions at $\sqrt{s_{\rm NN}} = 5.02$ TeV, Phys. Lett. B **726**, 164 (2013).

[41] V. Khachatryan *et al.* (CMS Collaboration), Long-range two-particle correlations of strange hadrons with charged particles in pPb and PbPb collisions at LHC energies, Phys. Lett. B **742**, 200 (2015).

[42] V. Khachatryan *et al.* (CMS Collaboration), Evidence for Collective Multi-Particle Correlations in pPb Collisions, Phys. Rev. Lett. **115**, 012301 (2015).

[43] M. Aaboud *et al.* (ATLAS Collaboration), Measurement of multi-particle azimuthal correlations in pp, $p+$Pb and low-multiplicity Pb + Pb collisions with the ATLAS detector, Eur. Phys. J. C **77**, 428 (2017).

[44] M. Aaboud *et al.* (ATLAS Collaboration), Measurement of long-range multiparticle azimuthal correlations with the subevent cumulant method in pp and $p+Pb$ collisions with the ATLAS detector at the CERN Large Hadron Collider, Phys. Rev. C **97**, 024904 (2018).

[45] C. Aidala *et al.* (PHENIX Collaboration), Creation of quark-gluon plasma droplets with three distinct geometries, Nat. Phys. **15**, 214 (2019).

[46] L. Adamczyk *et al.* (STAR Collaboration), Long-range pseudorapidity dihadron correlations in $d+$Au collisions at $\sqrt{s_{\rm NN}} =$ 200 GeV, Phys. Lett. B **747**, 265 (2015).

[47] A. Adare *et al.* (PHENIX Collaboration), Measurements of Elliptic and Triangular Flow in High-Multiplicity ^{3}He+Au Collisions at $\sqrt{s_{\rm NN}} = 200$ GeV, Phys. Rev. Lett. **115**, 142301 (2015).

[48] C. Aidala *et al.* (PHENIX Collaboration), Measurements of Multiparticle Correlations in $d+$Au Collisions at 200, 62.4, 39, and 19.6 GeV and $p+$Au Collisions at 200 GeV and Implications for Collective Behavior, Phys. Rev. Lett. **120**, 062302 (2018).

[49] K. Dusling, W. Li, and B. Schenke, Novel collective phenomena in high-energy proton-proton and proton-nucleus collisions, Int. J. Mod. Phys. E **25**, 1630002 (2016).

[50] J. L. Nagle and W. A. Zajc, Small system collectivity in relativistic hadronic and nuclear collisions, Annu. Rev. Nucl. Part. Sci. **68**, 211 (2018).

[51] B. Schenke, C. Shen, and P. Tribedy, Running the gamut of high energy nuclear collisions, Phys. Rev. C **102**, 044905 (2020).

[52] F. Becattini, A thermodynamical approach to hadron production in e^+e^- collisions, Z. Phys. C **69**, 485 (1996).

[53] F. Becattini, P. Castorina, J. Manninen, and H. Satz, The thermal production of strange and non-strange hadrons in e^+e^- collisions, Eur. Phys. J. C **56**, 493 (2008).

[54] P. Castorina, D. Kharzeev, and H. Satz, Thermal hadronization and Hawking-Unruh radiation in QCD, Eur. Phys. J. C **52**, 187 (2007).

[55] P. Braun-Munzinger, J. Stachel, J. P. Wessels, and N. Xu, Thermal equilibration and expansion in nucleus-nucleus collisions at the AGS, Phys. Lett. B **344**, 43 (1995).

[56] S. Hawking, Particle creation by black holes, Commun. Math. Phys. **43**, 199 (1975); **46**, 206 (1976).

[57] W. Unruh, Notes on black hole evaporation, Phys. Rev. D **14**, 870 (1976).

[58] D. E. Kharzeev and E. M. Levin, Deep inelastic scattering as a probe of entanglement, Phys. Rev. D **95**, 114008 (2017).

[59] J. Berges, S. Floerchinger, and R. Venugopalan, Thermal excitation spectrum from entanglement in an expanding quantum string, Phys. Lett. B **778**, 442 (2018).

[60] A. M. Kaufman, M. E. Tai, A. Lukin, M. Rispoli, R. Schittko, P. M. Preiss, and M. Greiner, Quantum thermalization through entanglement in an isolated many-body system, Science **353**, 794 (2016).

[61] O. K. Baker and D. E. Kharzeev, Thermal radiation and entanglement in proton-proton collisions at energies available at the CERN Large Hadron Collider, Phys. Rev. D **98**, 054007 (2018).

[62] Z. Tu, D. E. Kharzeev, and T. Ullrich, Einstein-Podolsky-Rosen Paradox and Quantum Entanglement at Subnucleonic Scales, Phys. Rev. Lett. **124**, 062001 (2020).

[63] A. Badea, A. Baty, P. Chang, G. M. Innocenti, M. Maggi, C. McGinn, M. Peters, T.-A. Sheng, J. Thaler, and Y.-J. Lee, Measurements of Two-Particle Correlations in e^+e^- Collisions at 91 GeV with ALEPH Archived Data, Phys. Rev. Lett. **123**, 212002 (2019).

[64] I. Abt *et al.* (ZEUS Collaboration), Two-particle azimuthal correlations as a probe of collective behaviour in deep inelastic ep scattering at HERA, J. High Energy Phys. 04 (2020) 070.

[65] A. H. Mueller, Multiplicity and hadron distributions in QCD jets: Nonleading terms, Nucl. Phys. B **213**, 85 (1983).

[66] M. Cacciari, G. P. Salam, and G. Soyez, The anti-k_t jet clustering algorithm, J. High Energy Phys. 04 (2008) 063.

[67] T. Sjöstrand, S. Mrenna, and P. Z. Skands, A brief introduction to PYTHIA 8.1, Comput. Phys. Commun. **178**, 852 (2008).

[68] G. Aad *et al.* (ATLAS Collaboration), Measurement of the charged-particle multiplicity inside jets from $\sqrt{s} = 8$ TeV pp collisions with the ATLAS detector, Eur. Phys. J. C **76**, 322 (2016).

[69] P. Koch, B. Muller, and J. Rafelski, Strangeness in relativistic heavy ion collisions, Phys. Rep. **142**, 167 (1986).

[70] J. Adam *et al.* (ALICE Collaboration), Enhanced production of multi-strange hadrons in high-multiplicity proton-proton collisions, Nat. Phys. **13**, 535 (2017).

[71] G. Gatoff and C. Y. Wong, Origin of the soft p(T) spectra, Phys. Rev. D **46**, 997 (1992).

[72] R. Hagedorn, Statistical thermodynamics of strong interactions at high-energies, Nuovo Cim. Suppl. **3**, 147 (1965).

[73] V. Khachatryan *et al.* (CMS Collaboration), Multiplicity and rapidity dependence of strange hadron production in pp, pPb, and PbPb collisions at the LHC, Phys. Lett. B **768**, 103 (2017).

[74] S. Acharya *et al.* (ALICE Collaboration), Multiplicity dependence of π, K, and p production in pp collisions at $\sqrt{s} = 13$ TeV, Eur. Phys. J. C **80**, 693 (2020).

[75] B. B. Abelev *et al.* (ALICE Collaboration), Multiplicity dependence of pion, kaon, proton and Lambda production in p-Pb collisions at $\sqrt{s_{NN}} = 5.02$ TeV, Phys. Lett. B **728**, 25 (2014).

[76] R. Hanbury Brown and R. Q. Twiss, A test of a new type of stellar interferometer on Sirius, Nature (London) **178**, 1046 (1956).

[77] W. A. Zajc *et al.*, Two pion correlations in heavy ion collisions, Phys. Rev. C **29**, 2173 (1984).

[78] U. W. Heinz and B. V. Jacak, Two particle correlations in relativistic heavy ion collisions, Annu. Rev. Nucl. Part. Sci. **49**, 529 (1999).

[79] M. A. Lisa, S. Pratt, R. Soltz, and U. Wiedemann, Femtoscopy in relativistic heavy ion collisions, Annu. Rev. Nucl. Part. Sci. **55**, 357 (2005).

[80] A. Adare *et al.* (PHENIX Collaboration), Enhanced Production of Direct Photons in Au + Au Collisions at $\sqrt{s_{NN}} = 200$ GeV and Implications for the Initial Temperature, Phys. Rev. Lett. **104**, 132301 (2010).

[81] J. Adam *et al.* (ALICE Collaboration), Direct photon production in Pb-Pb collisions at $\sqrt{s_{\rm NN}} = 2.76$ TeV, Phys. Lett. B **754**, 235 (2016).

[82] L. Adamczyk *et al.* (STAR Collaboration), Direct virtual photon production in Au + Au collisions at $\sqrt{s_{NN}} = 200$ GeV, Phys. Lett. B **770**, 451 (2017).

[83] D. Bertolini, T. Chan, and J. Thaler, Jet observables without jet algorithms, J. High Energy Phys. 04 (2014) 013.

[84] A. J. Larkoski, D. Neill, and J. Thaler, Jet shapes with the broadening axis, J. High Energy Phys. 04 (2014) 017.